Ultrafast carrier-carrier scattering among photoexcited nonequilibrium carriers in GaAs

M. G. Kane, K. W. Sun, and S. A. Lyon
Department of Electrical Engineering, Princeton University, Princeton, New Jersey 08544
(Received 7 February 1994)

We have studied carrier-carrier scattering in photoexcited electron-hole plasmas in GaAs at plasma densities from 10^{15} to 10^{17} cm^{-3}, using numerical solution of the dynamically screened Boltzmann equation and classical molecular dynamics. The solution of the dynamically screened Boltzmann equation indicates that for excited electrons, scattering among the injected carriers is as important a scattering process as LO-phonon emission at densities greater than about 8×10^{15} cm^{-3}, and at 10^{17} cm^{-3} the photoexcited electrons are nearly thermalized in 150 fsec. As a result of weaker screening, the interaction between carriers has a stronger effect in this case than when a low density of energetic electrons is immersed in a cool background plasma, where previous work has shown that carrier-carrier scattering becomes as significant as LO-phonon emission at a density of about 8×10^{16} cm^{-3}. We also find that classical molecular-dynamics calculations are dominated by nonphysical effects at short times, arising from the pointlike nature of the simulated carriers.

I. INTRODUCTION

Typical photoexcitation experiments use a continuous-wave or pulsed laser to create a distribution of energetic carriers having a narrow energy spectrum. These studies are complicated by the fact that carrier-carrier scattering (CCS) can rapidly modify the initial narrow distribution. Similar complications can arise in proposed hot electron transistor structures, which in the absence of the carrier-carrier interaction would permit quasiballistic transport of high-velocity carriers across a short base region. Here we consider the effects of CCS on energetic ($\geq$ 100 meV) Γ-valley electrons in a typical polar semiconductor, GaAs, at carrier densities from 10^{15} to 10^{17} cm^{-3}.

A distribution of energetic electrons undergoes rapid changes not only because of interactions between carriers but also through the emission of small-wave-vector LO phonons. (At energies greater than about 300 meV, electrons can also scatter to the upper valleys of the conduction band, but we will not consider this process.) LO-phonon emission causes discrete energy losses in multiples of the LO-phonon energy $\hbar\omega_{\mathrm{LO}} = 37$ meV. As a result, at low densities, where the carrier-carrier interaction is weak, an initially narrow distribution evolves into a series of peaks separated by $\hbar\omega_{\mathrm{LO}}$.[1] In bulk GaAs the LO-phonon emission time is about 150 fsec, relatively unaffected by electron energy or carrier density at our densities.[2–4]

The initial unrelaxed peak (or peaks) in the electron distribution represents electrons that have not yet emitted a LO phonon. The probability is small that an electron will be scattered out of this initial energy range before emitting a LO phonon if, during a LO-phonon emission time, scattering transfers little energy among carriers relative to the width of this peak. Thus at low densities the unrelaxed peak will be unaffected by CCS. At higher densities, however, the interactions will be stronger, and at sufficiently high densities CCS will reduce the height of the unrelaxed peak. The height of the unrelaxed peak thus allows us to compare the relative importance of CCS and LO-phonon emission for the scattering of energetic electrons.

The case of energetic electrons scattering from a cool equilibrium or quasiequilibrium background of carriers has been studied both experimentally and theoretically. In the presence of a cool background plasma the unrelaxed peak height is reduced by one-half at a plasma density of approximately 8×10^{16} cm^{-3}.[5–7] This is therefore the background density at which CCS begins to compete with LO-phonon emission for the scattering of energetic electrons in bulk GaAs. A very different situation is one where energetic carriers in a nonequilibrium distribution scatter only among themselves, with no cool background present. This corresponds to an experiment where all the carriers are generated by a laser pulse of length $\leq$ 150 fsec (the LO-phonon emission time), and a time-resolved measurement of the distribution is made during the first few hundred femtoseconds after the carriers are generated. This type of experiment is difficult to perform, since signal-to-noise problems make time-resolved techniques difficult at carrier densities below about 10^{17} cm^{-3}. However, experiments have shown that, in the absence of a cool background in bulk GaAs, the unrelaxed peak height is reduced by one-half at an injected pair density of approximately 8×10^{15} cm^{-3},[8] and at a density of 1.7×10^{17} cm^{-3} the photoexcited carriers spread out over a wide range of energies within 100 fsec.[9] These experiments suggest that in the absence of a cool background CCS begins to compete with LO-phonon emission at a lower density than when a cool background is present.

It is reasonable that scattering among carriers will be stronger in the absence of a cool background, since

screening is weaker in an energetic nonequilibrium distribution than in a cool thermal one. Early experimental evidence of this fact was provided by time-resolved Raman spectroscopy of optically pumped GaAs, which showed that the screening of LO phonons that occurs at high carrier densities ($\geq 10^{18}$ cm^{-3}) does not develop until the high-energy optically injected screening carriers have had time to cool and thermalize.[4] A first estimate of the screening difference between an energetic nonequilibrium distribution and a cool thermal one can be obtained by comparing the electron screening lengths. We model the photoexcited electron distribution as an isotropic shell in k space, with density n at energy $E = \hbar^2 k^2/2m^*$. In the random-phase approximation the static dielectric function for this distribution is

$$\epsilon_{\text{shell}}(q,0) = \epsilon_0 + \frac{4\pi n e^2 m^*}{\hbar^2 q^3 k} \ln\left[\frac{2k+q}{2k-q}\right] \approx \epsilon_0\left(1 + \frac{q_{\text{shell}}^2}{q^2}\right), \quad (1)$$

where $1/q_{\text{shell}} = \lambda_{\text{shell}} = \sqrt{\epsilon_0 E/2\pi n e^2}$ is the screening length for the shell distribution, and the approximation holds in the long-wavelength limit. In the same limit the static dielectric function of an equilibrium distribution with average energy $\bar{E}$ has the same form, but with a different screening length. For a Fermi distribution the screening length has the Thomas-Fermi value $\lambda_{\text{TF}} = \sqrt{5\epsilon_0 \bar{E}/18\pi n e^2}$, where we have used the zero-temperature relation between the average energy and the Fermi energy, $\bar{E} = 3E_F/5$. For a Maxwell-Boltzmann distribution the screening length has the Debye value $\lambda_D = \sqrt{\epsilon_0 \bar{E}/6\pi n e^2}$, where we have used $\bar{E} = 3kT/2$. The screening lengths of the three distributions exhibit the same dependence on density and average energy (as do all isotropic three-dimensional distributions), but differ by a constant factor that depends weakly on the shape of the distribution. For a given density and average energy, the screening lengths for the shell, Fermi and Maxwell-Boltzmann distributions have the ratios 1.73:1.29:1. (Of course, in a given material a shell distribution and a Maxwell-Boltzmann distribution having the same density and average energy can be produced, but not a Fermi distribution.) Calculations using a static screening model have shown that the thermalization of a photoexcited distribution proceeds more rapidly when the calculations use the self-consistent screening length instead of the smaller Debye length.[10] The energy dependence of the screening length is more significant than the shape dependence, since in typical photoexcitation experiments the energy of the photoexcited electrons is much larger than the average electron energy in a background plasma. For energetic electrons at 150 meV, the ratio of the two energies can range from about 12 for a 100 K Maxwell-Boltzmann background to more than 250 for a low-density 4 K background. Therefore, in addition to the weak dependence of screening length on the shape of the distribution, the energy dependence introduces an additional factor ranging from about 3 to 15. The combined effect gives a nonequilibrium photoexcited electron distribution a screening length 5–25 times larger than a typical background. (In two dimensions the screening length depends more strongly on the shape of the carrier distribution.)

In this paper we will confirm this plausibility argument for stronger CCS in the absence of a cool carrier background. We model a typical experiment in which electron-hole pairs are generated in GaAs by 1.7 eV photons having an 18 meV full width at half maximum (FWHM), and measurements are made of the electron distribution. For initial conditions, the holes are partitioned between the valence bands in accordance with the relative photoexcitation probabilities $P_{\text{hh}} = 0.7$, $P_{\text{lh}} = 0.3$, with energies $E_{\text{hh}} = 21$ meV, $E_{\text{lh}} = 86$ meV. The electron distribution has two peaks, at 160 meV and 95 meV, corresponding to electrons promoted from the heavy-hole and light-hole bands, respectively. The initial energy width of each peak is determined from the spectral width of the excitation pulse and the shape of the conduction and valence bands. In our calculations we use initial widths of 20 meV and 12 meV FWHM for the high- and low-energy electron peaks, respectively. We calculate the dynamics of the electrons and holes for 150 fsec, the LO-phonon emission time. For the dynamics all bands are treated as parabolic and isotropic, using standard band-edge effective masses.[11] The relative importance of carrier-carrier interactions compared to LO-phonon emission for the scattering of the photoexcited electrons is determined by examining the higher-energy unrelaxed peak in the electron distribution after 150 fsec. We will show that in the absence of a cool background CCS is as significant a scattering mechanism as LO-phonon emission at pair densities greater than approximately 8×10^{15} cm^{-3}, and at 10^{17} cm^{-3} the photoexcited electrons are nearly thermalized in 150 fsec. Thus our calculations will confirm that CCS is stronger in this case than when a low density of energetic electrons is immersed in a cool background.

Previous calculations have not attempted to determine the density at which scattering among photoexcited carriers becomes comparable to LO-phonon emission. Lugli and Ferry used Monte Carlo calculations to compare CCS and LO-phonon emission in GaAs at a density of 10^{17} cm^{-3}, and found that after 200 fsec the initial electron distribution is spread out over a wide range of energies, so that all features associated with discrete LO-phonon emission are swamped out.[12] Elsaesser and co-workers performed similar calculations using Monte Carlo methods, as well as molecular dynamics, and found that at a density of 1.7×10^{17} cm^{-3} scattering among the carriers spreads the initial distribution over a wide energy range within 100 fsec.[9] Numerical solution of the Boltzmann equation by Hunsche and co-workers showed electron thermalization within 200 fsec at densities from 2×10^{17} to 2×10^{18} cm^{-3}.[13] Monte Carlo and molecular-dynamics calculations by Rota and Lugli yielded similar results at a density of 10^{18} cm^{-3} in InP.[14] None of these studies explored lower densities in order to determine the density at which scattering among photoexcited carriers begins to compete with LO-phonon scattering.

Most CCS calculations treat the interaction between carriers as statically screened using the static dielectric

function $\epsilon(\mathbf{q},0)$ as an approximation to the dynamic dielectric function $\epsilon(\mathbf{q},\omega)$. That is, the inertia of the screening carriers is ignored and screening is treated as instantaneous. This is a commonly used approach for two-dimensional[15–17] and three-dimensional[18–25] carrier systems. Plasmons are excluded from the static model, both as a channel for real energy losses and as a virtual excitation affecting collisions between carriers. Sometimes energy loss to plasmons is included as an additional scattering mechanism, so that CCS is treated in two parts, one part representing statically screened binary collisions and the other representing plasmon emission.[12,14,26–28] However, this still omits dynamic screening of the binary collisions. Static screening will be a poor approximation for any collision where the center-of-mass velocity is on the order of, or greater than, the velocity of the screening carriers.[29] Therefore a static screening model is not expected to yield accurate results in calculations of scattering among photoexcited carriers.

In the case of screening by holes, under some conditions one can justify using the high-frequency limit (rather than the static limit), simply ignoring the holes and regarding them as infinitely sluggish. However, this approximation does not hold with sufficient generality to employ it in our calculations. Furthermore, as a rule the electron screening can be treated in neither a static nor a high-frequency limit. Therefore we wish to avoid both the static and high-frequency approximations, and to treat both electron and hole screening dynamically.

In order to include dynamic screening, calculations of CCS have been performed using the dynamic dielectric function $\epsilon(\mathbf{q},\omega)$. Most of these studies consider the scattering rate of an energetic carrier immersed in a cool (or cold) equilibrium background.[6,7,30–34] In this case, when scattering is dominated by an equilibrium distribution, the fluctuation-dissipation theorem permits the carrier's scattering rate to be calculated from $\mathrm{Im}[\epsilon^{-1}(\mathbf{q},\omega)]$.[35] No other assumptions are made apart from treating the coupling between the energetic carrier and the background using the Born approximation, and the assumptions that enter into the calculation of the dielectric function itself. These calculations have shown that a dynamic screening model predicts significantly more scattering than is predicted by a static screening model.

Unfortunately, this equilibrium method is not applicable to the problem of photoexcited carriers scattering among themselves. In this case the fluctuation-dissipation theorem cannot be applied because scattering is not dominated by an equilibrium distribution. Nonequilibrium methods of calculation that include dynamic screening are required. Molecular dynamics is one such method; it has been applied to CCS by a number of researchers.[9,14,22,36,37] An alternative is to numerically solve the dynamically screened Boltzmann equation; the first calculations to use this method have represented dynamic screening in the simplified form of the plasmon-pole approximation.[13,38,39]

Here we apply these two nonequilibrium methods to the problem of scattering among photoexcited carriers. In Sec. II we discuss molecular dynamics and demonstrate that this method is contaminated by nonphysical effects at short times. In Sec. III we describe numerical solution of the Boltzmann equation, with dynamic screening included in the random-phase approximation. We show that the latter method successfully reproduces experimental results and provides insights into carrier-carrier scattering. In Sec. IV we summarize our results.

II. MOLECULAR-DYNAMICS CALCULATIONS

A. General method

Molecular dynamics (MD) is a numerical method for studying the behavior of interacting many-body systems. In MD calculations of CCS the true quantum dynamics is approximated by following the classical real-space trajectories of a large number of pointlike carriers. Each carrier interacts with all of the others via a bare Coulomb potential. The primary benefit of MD is that it includes classical dynamic screening. Screening is not treated explicitly, but rather arises naturally among the simulated carriers in a self-consistent manner as they execute their classical trajectories.

MD calculations of CCS rely on the fact that classical dynamics, applied to point particles, yields the correct Rutherford differential cross section for pure $1/r$ Coulomb scattering between two carrier plane waves (neglecting exchange).[40] Then the scattering of one carrier from all the others is the sum of the individual scattered intensities as long as the other carriers' positions are uncorrelated so that scattering amplitudes combine incoherently. In reality, the positions of the other carriers are correlated at long ranges; this screening of the long-range Coulomb potential is what prevents the total cross section from becoming infinite. The overall effect of this deviation from a pure Coulomb potential is that a classical calculation will slightly overestimate the total scattering rate. A rough indication of the classical overestimate can be obtained by considering an approximate expression for the energy loss of an electron with energy E to statically screened electron collisions in a cool plasma of density n:[41]

$$\frac{dE}{dx} \approx -\frac{2\pi n e^4}{\epsilon E}\ln\left[\frac{\lambda}{b_{\min}}\right], \tag{2}$$

where λ is the screening length in the plasma, and $b_{\min}$ is the so-called "minimum impact parameter." Classically $b_{\min}$ is $e^2/\epsilon E$, but quantum mechanically it can be no smaller than the positional uncertainty in the center-of-mass frame $\Delta x = 2/k$, where k is the wave number of the energetic electron. When E is larger than about 5 meV (the exciton Rydberg in GaAs), as it is for the cases of interest, the quantum-mechanical $b_{\min}$ exceeds the classical $b_{\min}$, and the classical model overestimates the energy loss. The ratio of classical to quantum-mechanical energy loss is therefore approximately

$$\ln\left[\frac{\lambda\epsilon E}{e^2}\right] : \ln\left[\frac{\lambda}{2}\sqrt{\frac{2m^*E}{\hbar^2}}\right], \tag{3}$$

which is less than 1.5 for the cases of interest. Although this ratio applies to energy loss through collisions with electrons in a cool plasma, we expect the classical model in MD to overestimate the effects of scattering among energetic carriers by roughly the same factor.

MD also treats plasmon scattering properly. Although plasma wave energies remain unquantized in MD, so that discrete plasmon emission cannot be reproduced, the plasmon energy at our densities is less than 15 meV, much smaller than the energy of the photoexcited electrons. Therefore, by the correspondence principle, the total energy-loss rate to plasma waves will be approximately the same with or without energy quantization.

In our MD calculations, care has been taken to avoid pitfalls that can threaten real-space simulations. We employ a second-order time integration scheme, and a time step of 0.2 fsec permits the total energy of the carrier system to be conserved to an accuracy better than 0.1% over the simulation period. Periodic boundary conditions are applied to the potential and the motion of the particles in order to minimize the effects of the finite simulation volume. We simulate a total of 2048 electrons and 2048 holes, so that the simulation volume is at least several screening lengths on a side. Since the simulation time is short, problems associated with classical bound states of electrons and holes do not arise. Electron-hole pairs are introduced at random positions, with a fixed electron-hole separation that is small compared to the average interpair distance. Each carrier thus starts with a well-defined kinetic and total energy. The MD calculations are performed on a MasPar MP-1 massively parallel computer with 4096 processors.

B. Results and problems with molecular dynamics

In our MD calculations the carriers interact for 150 fsec, corresponding to the LO-phonon emission time. Figure 1 shows the initial and final distribution of electron kinetic energies at pair densities from 10^{15} to 10^{17} cm^{-3}. The dependence of the peak-height reduction on density can be observed in this figure.

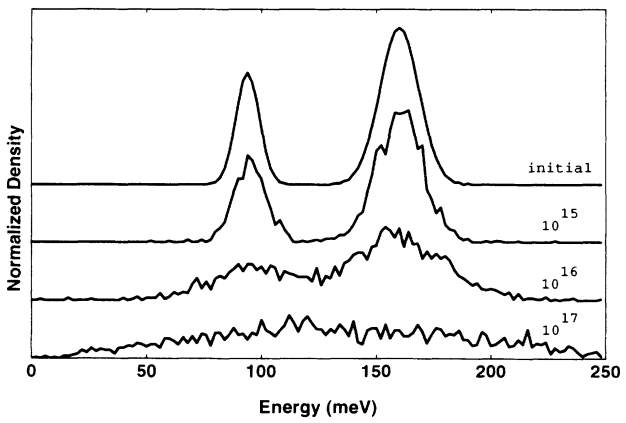

FIG. 1. The initial and final distribution of electrons in a photoexcited plasma at pair densities from 10^{15} to 10^{17} cm^{-3}, as calculated by molecular-dynamics simulations for 150 fsec. The two electron peaks represent electrons promoted from the heavy-hole and light-hole bands. All distributions are normalized to the total density.

However, a fundamental problem exists with the MD results. For the densities examined here, the calculated broadening is dominated by large potential fluctuations arising from the pointlike character of the simulated carriers. This breakdown of the classical model can easily be seen in a simulation using as an initial state the final 10^{16} cm^{-3} state from the calculations of Fig. 1, so that artifacts associated with initial conditions are avoided. We now continue the MD calculations for an additional 150 fsec, but with all carriers fixed except for one moving electron, so that the total energy of that electron is constant (which we verify). We perform an ensemble of such static scattering calculations, and compare the results to MD calculations that use the same initial state but permit all the carriers to move for the additional 150 fsec simulation. At the end of the calculations we measure the change in each electron's kinetic energy ΔE_K during the additional 150 fsec interval. Figure 2 shows the ΔE_K distribution for the static and dynamic calculations. The statically broadened distribution is only slightly narrower than the distribution obtained using dynamic calculations, demonstrating that the broadening that occurs in 150 fsec is dominated by static effects. Most of the static broadening arises from interactions at distances less than 250 Å, while all of the carriers in these photoexcitation experiments must exist as rather large wave packets (at least 1000 Å) to be consistent with the energy width of the laser pulse.

These observations are consistent with the remarks in Sec. II A about the accuracy of the classical model used in MD, since those statements applied to the asymptotic behavior of the scattered carriers. The potential energy

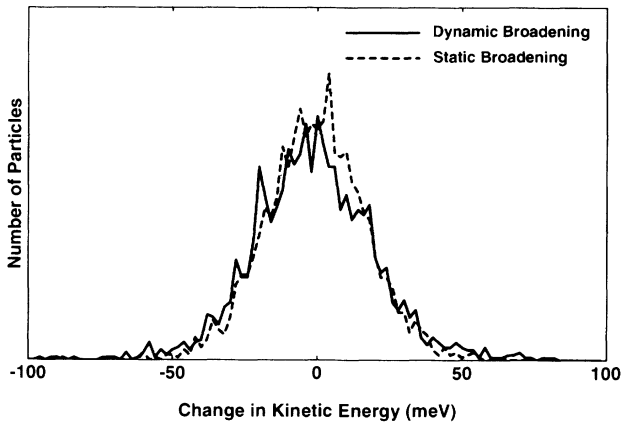

FIG. 2. The distribution of the change in electron kinetic energy ΔE_K after 150 fsec, calculated by molecular dynamics with all particles moving (dynamic broadening), and with only one particle moving (static broadening). The initial distribution is the final 10^{16} cm^{-3} distribution from Fig. 1. The statically broadened distribution is only slightly narrower than the distribution obtained using dynamic calculations, demonstrating that in molecular dynamics the broadening that occurs in 150 fsec is dominated by static effects.

fluctuations created by the classical point particles are much larger than those generated by large wave packets. As a result, during an initial time period after photoexcitation, most of the change in the kinetic energy of pointlike carriers is due not to completed collisions, but to the spread in kinetic energies that occurs during collisions. It is only after an initial period, when many collisions have been completed, that the broadening due to potential fluctuations saturates, and the spread in kinetic energies represents completed energy transfers between carriers. Then classical dynamics will yield more accurate results. Our MD calculations show that, in the first 150 fsec at densities $\leq 10^{17}$, the spread in kinetic energies calculated by MD is strongly influenced by the static component. We conclude that the predictions of MD are contaminated by nonphysical broadening arising from treating the carriers as point particles.

Several studies have noted that MD predicts higher CCS rates at short times than static screening calculations, and have attributed the difference to the more accurate dynamic screening included in MD.[9,22,28] However, our observations indicate that the differences observed in these studies may partly reflect the nonphysical broadening that occurs in MD.

It is tempting to graft onto MD a quantum-mechanical softening of the $1/r$ potential in order to prevent the spurious broadening. Effective pair potentials have been employed in studies of plasmas to eliminate the troublesome classical Coulomb divergence at $r = 0$,[42–44] and they have been applied to MD by Hansen and coworkers.[45] However, these formulations assume an equilibrium electron distribution, so that they are not applicable to our problem. Similar restrictions apply to the *ab initio* molecular-dynamics method developed by Car and Parrinello.[46,47] An alternative approach to softening the potential that does not assume an equilibrium distribution has been proposed by Kriman and co-workers.[48,49] They model the carriers as spherical Gaussian wave packets with a specified fixed size, and modify the potential between particle centers so that it represents the interaction between two spherical charge clouds. However, as noted above, our carrier wave packets must be quite large in order to be consistent with the energy width of our laser pulse. As a result substantial wave-function overlap exists, and the interaction between packets cannot be treated adequately in terms of a classical field between charge clouds. (If the interaction could be represented as a classical field, then in the limit of very large clouds—two plane waves—there would be only $q = 0$ scattering, whereas the quantum-mechanical interaction between plane waves has a $1/q^2$ dependence, permitting scattering over a range of q values.)

Furthermore, even if a potential could be devised that correctly represents the interaction between quantum-mechanical wave packets, point particles moving in well-defined orbits can be used with a potential representing wave-packet interactions only if wave-packet dispersion during scattering can be neglected. The Coulomb scattering of two wave packets can be treated as dispersionless only when the classical "minimum impact parameter" $e^2/2\epsilon E_{\rm CM}$ exceeds the uncertainty in the center-of-mass frame $\Delta x = 1/k_{\rm CM}$.[40,50] (Here $E_{\rm CM}$ is the total energy in the center-of-mass frame, and $k_{\rm CM}$ is the corresponding wave number for a particle with the reduced mass.) Otherwise wave-packet dispersion during scattering renders orbital pictures inappropriate. In GaAs this condition is met only for collisions where $E_{\rm CM}$ is less than about 5 meV, the exciton Rydberg. Therefore modification of the $1/r$ potential is not expected to yield an accurate differential cross section for most of the carrier-carrier collisions in a photoexcited plasma.

III. THE BOLTZMANN EQUATION WITH DYNAMIC SCREENING

A. Dynamic screening and the dielectric function

We have seen that MD calculations of CCS encounter problems arising from the difficulty of simultaneously (1) correctly representing the differential scattering cross section for a collision between two carriers and (2) correctly representing the broadening that occurs during collisions. This is a dilemma arising from the classical model used in MD, and it can be overcome only by abandoning classical dispersion-free orbits. An exact solution using time integration of the many-body Schrödinger equation is the quantum-mechanical equivalent of classical MD, with dynamic screening arising naturally as constructive and destructive interference occurs among the scattering amplitudes. However, solving the Schrödinger equation exactly is intractable for our plasmas.

Various approximations can be applied to the quantum-mechanical treatment of CCS in order to render it tractable. In the Hartree and Hartree-Fock approximations each carrier moves in a mean potential due to all the others. However, in our plasmas the electron and hole wave packets are quite large and substantial overlap exists among them, so that the mean potential is small and cannot reproduce the binary collisions that occur between carriers. To confirm this observation, we have performed many-body time-dependent Hartree calculations of the carrier-carrier dynamics, using as initial wave functions Gaussian wave packets with sizes consistent with the energy width of the laser pulse. The results show very weak scattering, confirming that the carrier-carrier interaction is underestimated in the Hartree approximation.

The problem with using a classical field operating on quantum-mechanical wave functions to calculate the effects of CCS is not the treatment of screening: time-dependent Hartree screening is equivalent to screening in the random-phase approximation (RPA),[51] but without assumptions concerning linearity and stationarity. Rather, the problem is that the classical field induced by the charge density of a smeared-out carrier is weak within the carrier's charge cloud. Therefore, as noted in Sec. II B, when substantial wave-function overlap exists, as it does here, a classical field cannot adequately represent the interaction between carriers. (This is particularly clear in the case of plane waves.) To represent

the interaction accurately, we return to the bare $4\pi e^2/q^2$ Coulomb interaction between each pair of carrier wave functions. Because it is impossible to keep track of the many-body state of the system, dynamic screening is introduced *ab extra* using the longitudinal dynamic dielectric function $\epsilon(\mathbf{q},\omega)$.

For a general time-dependent carrier distribution the dielectric function is nonstationary. If the dielectric function varies significantly during the time in which a collision takes place, the collision is governed by a time-dependent Hamiltonian, and calculations are difficult. For the cases that we are considering, a collision period is typically 100 fsec or less, and the dielectric function does not vary strongly during this length of time, i.e., it is stationary in a first approximation. Indeed, it varies little over the entire 150 fsec simulation period, so that it only needs to be calculated at the beginning of the period. The approximate stationarity of the dielectric function arises from constraints that exist along both the frequency axis and the wave-vector axis; that is, $\epsilon(\mathbf{q},\omega)$ is constrained by requirements on both $\lim_{q\to 0}\epsilon(\mathbf{q},\omega)$ and $\epsilon(\mathbf{q},0)$. Along the frequency axis, the zero at the plasma frequency does not move significantly as the distribution evolves in time, because the plasma frequency is primarily a function of the density and effective mass of each carrier type. Along the wave-vector axis the static screening wave number increases by only a small factor as the distribution evolves, because, as noted in Sec. I, the screening length depends primarily on the density and average energy of each carrier type, rather than the shape of the carrier distributions, but the densities and average energies vary little in 150 fsec. Energetic electrons can emit approximately one LO phonon in 150 fsec; energetic holes may be able to emit optical phonons faster than this,[52] but most of the holes in our plasmas are heavy holes with less than 25 meV energy, which is below the threshold for emitting optical phonons.

Using the approximation that the dielectric function is stationary, it is possible to perform a tractable CCS calculation that includes dynamic screening. For the range of energies and densities that we consider here, the photoexcited electrons have kinetic energies that far exceed their average potential energy $e^2n^{1/3}/\epsilon_0$, so that they are weakly coupled to the carrier system, allowing the RPA dielectric function to be used.[35]

The dielectric function is complex, with an imaginary part that represents energy exchanged with the dielectric medium through dissipative processes, including plasmon emission and absorption, as well as LO-phonon scattering (since the Fröhlich lattice susceptibility is also included in the dielectric function). Since we use the dielectric function only to provide dynamic screening of the binary collisions, we do not include these dissipative processes, which would require separate scattering calculations. It is reasonable that we ignore the effects of phonon scattering, because we are using the change in peak height over the 150 fsec simulation period in order to compare the importance of CCS and LO-phonon scattering. Furthermore, plasmon scattering needs to be considered only if the energy of the scattered electron is well above the average energy of the surrounding electrons.[53] Otherwise the plasmon modes are Landau damped by the surrounding electrons in the range of wave vectors in which the energetic electron is permitted by energy and momentum conservation to emit plasmons. In the absence of a cool electron background, this condition is not satisfied, since none of the electrons have energies significantly higher than average. Stability theory for isotropic plasmas,[54,55] as well as Monte Carlo calculations that include plasmon scattering,[12] confirm that this process is not significant among photoexcited carriers. We are therefore justified in neglecting plasmon scattering.

B. General method

To calculate scattering probabilities, we apply first-order time-dependent perturbation theory through the use of Fermi's golden rule, with a screened Coulomb potential as the perturbing potential. First-order perturbation theory can be applied to CCS if the classical "minimum impact parameter" $e^2/2\epsilon E_{\rm CM}$ is much less than the uncertainty in the center-of-mass frame $\Delta x = 1/k_{\rm CM}$, where $E_{\rm CM}$ is the total energy in the center-of-mass frame, and $k_{\rm CM}$ is the corresponding wave number for a particle with the reduced mass.[40,50] (This high-energy condition is exactly the opposite of the low-energy condition given in Sec. II B, under which classical, orbital pictures can be applied to the Coulomb scattering of two wave packets.) Therefore in GaAs first-order perturbation theory can be applied to collisions where $E_{\rm CM}$ is much greater than about 5 meV, the exciton Rydberg. In most of the carrier-carrier collisions in our plasmas $E_{\rm CM}$ is on the order of 150 meV, and this condition is satisfied.

Using Fermi's golden rule to calculate scattering rates, the evolution of the carrier distribution functions can be followed by numerically integrating the Boltzmann equation over time. Statically screened Boltzmann equation calculations of carrier-carrier scattering have been performed previously, using both Monte Carlo and deterministic methods in two-dimensional[15–17] and three-dimensional[14,18–25] carrier systems. Recently Collet and co-workers included dynamic screening in the plasmon-pole approximation in Boltzmann equation calculations of CCS.[13,38,39] Here we employ the full RPA dynamic dielectric function.

We include electron-electron and electron-hole scattering processes. The electron-hole scattering includes both intra-valence- and inter-valence-band scattering. For a collision that transfers momentum $\hbar q$ and energy $\hbar\omega$ between two carriers, the probability of scattering is calculated from the square of the matrix element $M(q,\omega) = 4\pi e^2/q^2\epsilon(q,\omega)$.[29] This matrix element does not include exchange effects, which are small at our densities. The probability of electron-hole scattering must include as an additional factor the squared overlap integral $G_{ij}(\mathbf{k},\mathbf{k}')$ between the initial hole state $\mathbf{k}$ in band i and the final hole state $\mathbf{k}'$ in band j. For intra-valence-band scattering $i=j$, and for inter-valence-band scattering $i\neq j$. We use the expressions for two-band overlap integrals obtained by Wiley,[56]

$$G_{ij}(\theta) = \begin{cases} \frac{1}{4}(1+3\cos^2\theta), & i=j \\ \frac{3}{4}\sin^2\theta, & i\neq j, \end{cases} \quad (4)$$

where θ is the angle between $\mathbf{k}$ and $\mathbf{k}'$. If the collision changes the hole momentum by $\hbar q$, this angle can be calculated using $\cos\theta = (k^2 + k'^2 - q^2)/2kk'$.

The dielectric function includes contributions from the dielectric susceptibilities of the carriers, as well as the frequency-dependent Fröhlich lattice susceptibility:

$$\epsilon(q,\omega) = \epsilon_\infty + \frac{\omega_{TO}^2(\epsilon_0-\epsilon_\infty)}{\omega_{TO}^2-\omega^2-i\gamma\omega} + 4\pi\sum_i \chi_i(q,\omega), \quad (5)$$

using standard values for the lattice parameters ϵ_0, ϵ_∞, ω_{TO}, and γ.[11] The carrier susceptibilities $\chi_i(q,\omega)$ are calculated from the initial hot carrier distribution using the Lindhard expression.[57] They include the effects of intraconduction, intravalence, and intervalence transitions.

The rate at which a carrier scatters out of a state $\mathbf{k}_1$ due to each scattering process is

$$\left.\frac{df(\mathbf{k}_1)}{dt}\right|_{out} = \frac{2\pi}{\hbar}\frac{g}{(2\pi)^6}\int d^3k_2 d^3k_3 d^3k_4\ |M(q,\omega)|^2\ G_{ij}(\theta) f(\mathbf{k}_1) f(\mathbf{k}_2)[1-f(\mathbf{k}_3)][1-f(\mathbf{k}_4)]$$
$$\times\ \delta(\mathbf{k}_1+\mathbf{k}_2-\mathbf{k}_3-\mathbf{k}_4)\ \delta(E_1+E_2-E_3-E_4), \quad (6)$$

where $g=2$ is the degeneracy of the colliding carriers, $\mathbf{k}_1$, $\mathbf{k}_2$, E_1, and E_2 are the wave vectors and energies of the initial states of colliding carriers 1 and 2, respectively, and $\mathbf{k}_3$, $\mathbf{k}_4$, E_3, and E_4 are the wave vectors and energies of their final states. The matrix element is evaluated at $q=|\mathbf{k}_3-\mathbf{k}_1|$ and $\omega=(E_3-E_1)/\hbar$. For electron-hole scattering $G_{ij}(\theta)$ is calculated from Eq. (4), while for electron-electron scattering it is set to unity. An analogous equation describes the scattering into the state $\mathbf{k}_1$. The complete nine-dimensional integral can be simplified considerably by performing several of the integrals analytically, taking advantage of the fact that we are modeling the distribution function as isotropic in k space. As shown by Snoke and co-workers,[25,58] only three wave-number integrals remain, and converting two of these to energy integrals yields

$$\left.\frac{dn(E_1)}{dt}dE_1\right|_{out} = \frac{2\pi}{\hbar}\frac{g^2}{(2\pi)^9}\frac{16\pi^3 m_1 m_2 m_3 m_4}{\hbar^{16}}\ dE_1\int_0^\infty dE_2\int_0^\infty dE_3$$
$$\times\int_{q_{min}}^{q_{max}} dq\ |M(q,\omega)|^2\ G_{ij}(\theta) f(E_1) f(E_2)[1-f(E_3)][1-f(E_4')], \quad (7)$$

where $n(E_1)dE_1$ is the density of carriers between E_1 and E_1+dE_1. The initial and final effective masses of carrier 1 are m_1 and m_3, which are different if this carrier is a hole undergoing an intervalence transition. Similarly, the initial and final effective masses of carrier 2 are m_2 and m_4. By energy conservation $E_4' = E_1+E_2-E_3$, with k_4' the corresponding wave number. The wave-number limits correspond to the minimum and maximum momentum transfers, $q_{min} = \max(|k_1-k_3|, |k_2-k_4'|)$ and $q_{max} = \min(k_1+k_3, k_2+k_4')$. If inter-valence-band scattering is not considered and a simple static screening model is employed, $G_{ij}(\theta)$ can be omitted, and $M(q,\omega)$ can be set to $4\pi e^2/\epsilon_0(q^2+q_s^2)$, where q_s is the screening wave number. Then the q integration can be performed analytically.[25] However, we must perform the q integration numerically because of the presence of $G_{ij}(\theta)$ for intervalence scattering, and because $M(q,\omega) = 4\pi e^2/q^2\epsilon(q,\omega)$, where $\epsilon(q,\omega)$ has been evaluated numerically.

The numerical integration of Eq. (7) is performed over a 250 meV range of electron and hole energies, using an energy interval of 2 meV, and a wave-number interval of 0.02–0.1 times the inverse static screening length. We have verified that the energy interval is sufficiently fine to permit the conductivity sum rule and the f-sum rule for the free-carrier dielectric function to be satisfied to an accuracy of better than ±10%:

$$\int_0^\infty d\omega\ \omega\ \mathrm{Im}[\epsilon(q,\omega)] = \frac{\pi}{2}\omega_p^2,$$
$$\int_0^\infty d\omega\ \omega\ \mathrm{Im}\left[\frac{1}{\epsilon(q,\omega)}\right] = -\frac{\pi}{2}\omega_p^2, \quad (8)$$

where ω_p is the plasma frequency, provided that the dielectric function is damped with a collisional damping time of 1 psec. Although we find that our results are unaffected when much longer damping times are used (since the results depend primarily on the real part of the dielectric function), we perform all our calculations with 1 psec damping in order to ensure that the sum rules are satisfied. The time integration is performed with a time step of 1–50 fsec for each iteration, depending on the scattering rate, and we verify total energy conservation as well as electron and hole conservation over the simulation period. A complete 150 fsec calculation requires from 5 to 50 h on a workstation.

C. Results

1. *Electron scattering in a photoexcited plasma*

Dynamically screened Boltzmann calculations were performed for electrons in a photoexcited plasma, with

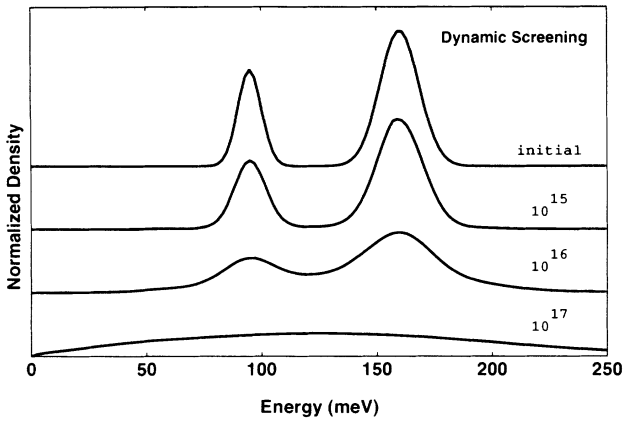

FIG. 3. The initial and final distribution of electrons in a photoexcited plasma at pair densities from 10^{15} to 10^{17} cm^{-3}, as calculated by integrating the dynamically screened Boltzmann equation for 150 fsec. The calculation includes intra-conduction-, intra-valence-, and inter-valence-band transitions. All distributions are normalized to the total density, and the baseline for each plot can be determined from the left-hand edge of the figure. The higher-energy electron peak height is reduced by one-half at a density of approximately 8×10^{15} cm^{-3}, and at 10^{17} cm^{-3} the final distribution is approaching but has not reached a hot Maxwell-Boltzmann.

the evolution of the electron distribution followed for 150 fsec, the LO-phonon emission time. Figure 3 shows the initial and final electron distribution at pair densities from 10^{15} to 10^{17} cm^{-3}. (Because of the large spread of the final distribution at 10^{17} cm^{-3}, the calculation was performed over a 500 meV energy range, of which only the lower half is shown.) The rate at which electrons are scattered out of the unrelaxed peak is equal to the LO-phonon scattering rate if CCS reduces the height of the initial distribution by one-half. By performing calculations at densities between those shown in Fig. 3, we find that for the higher-energy peak this occurs at a pair density of 8×10^{15} cm^{-3}. At 10^{17} cm^{-3} the final distribution is approaching but has not reached a hot Maxwell-Boltzmann, as can be seen from the fact that the peak of the distribution is at 125 meV, which is close to its average energy $\bar{E} = 130$ meV, but if the distribution were completely thermalized its peak would lie at 1/3 of the average energy, or 43 meV. These results agree with experimental results showing that, in the absence of a cool background, scattering among photoexcited carriers reduces the peak height by one-half at 8×10^{15} cm^{-3} ($\pm 50\%$),[8] and at 1.7×10^{17} cm^{-3} ($\pm 50\%$) the photoexcited electrons spread out over a wide range of energies within 100 fsec.[9]

Additional calculations were performed to determine the relative importance of the different hole scattering mechanisms. We find that scattering of electrons from the heavy holes is negligible because of the large mass difference. However, the light holes account for approximately 15% of the CCS, since their mass is slightly mismatched from the electron mass, and the light-hole density is 30% of the total pair density. [Light holes will be less important in an equilibrium plasma, where the fraction of light holes is determined by the ratio between the light-hole and heavy-hole density of states, so that the density of light holes is only $m_{\rm lh}^{3/2}/(m_{\rm hh}^{3/2} + m_{\rm lh}^{3/2}) = 6\%$ of the total pair density.] We find that inter-valence-band scattering is unimportant, because there is little hole occupation at the center of the Brillouin zone, where the heavy-hole and light-hole bands are degenerate. Since the overlap integral between the two valence bands, given in Eq. (4), introduces a $\sin^2\theta$ factor into the scattering probability (where θ is the scattering angle of the hole that changes bands),[56] inter-valence-band transitions involve large wave-vector changes, which are suppressed by the $1/q^2$ factor in the Coulomb matrix element; they also require large energy changes (tens of meV), so that they do not contribute to the dielectric function in the range of typical collisional energy transfers. Inter-valence-band scattering is more important in a cool plasma, as confirmed in calculations by Young and co-workers,[6,21] because the presence of holes at the zone center enhances the intervalence scattering rate, while stronger screening reduces the rate of intra-conduction-band scattering.

The dependence of CCS on the energy of the photoexcited electrons was also examined. The scattering rate increases sublinearly with increasing electron energy, due primarily to the increased screening length at higher energies. The effects of the scattering also depend on the initial energy width of the unrelaxed peak, since the wider the initial peak, the more slowly electrons are scattered out this energy window, and the more slowly the peak height drops.

2. *Electron scattering in a cool plasma*

For comparison, dynamically screened Boltzmann calculations were performed for the case of a low density of energetic carriers immersed in a 100 K Maxwell-Boltzmann plasma. The photoexcited carriers have the same initial conditions as for the former calculations, but they comprise only 1% of the total carrier density. Figure 4 shows the initial and final electron distribution at pair densities from 10^{15} to 10^{17} cm^{-3}. Calculations at densities between those in Fig. 4 show that electrons are scattered out of the higher-energy peak at a rate equal to the LO-phonon scattering rate at a pair density of 4×10^{16} cm^{-3}. This result falls at the lower end of the experimental range of 8×10^{16} cm^{-3} $\pm 50\%$ obtained by Kash.[5] One reason for the lower density obtained in our calculations is that we use an electron energy of 160 meV, while in Kash's experiment the energy is about 300 meV. We have performed additional calculations using a 300 meV electron energy in order to duplicate the parameters of Kash's experiment, and we find that the density at which carrier-carrier scattering is as significant as LO-phonon scattering is increased about 25%, to 5×10^{16} cm^{-3}. Thus the scattering rate has a weak inverse dependence on the electron energy when energetic electrons scatter in a cool plasma. In addition, we believe that our calculations of electron scattering in a cool plasma slightly underestimate the density at which

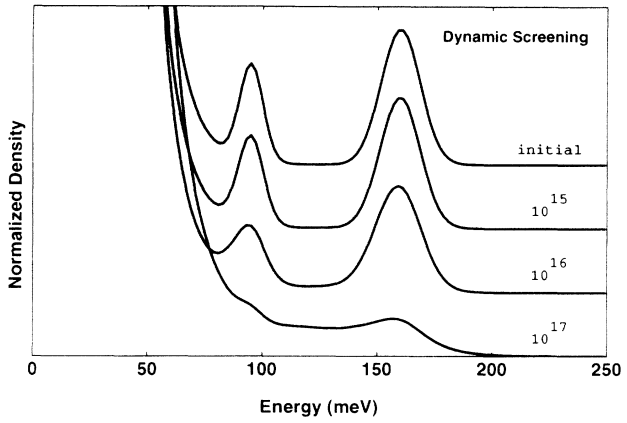

FIG. 4. The initial and final distribution of photoexcited electrons immersed in a 100 K Maxwell-Boltzmann plasma, calculated in the same manner as in Fig. 3. The photoexcited density is 1% of the total carrier density. The baseline for each plot can be determined from the right-hand edge of the figure. The peak height is reduced by one-half at a pair density of approximately 4×10^{16} cm^{-3}.

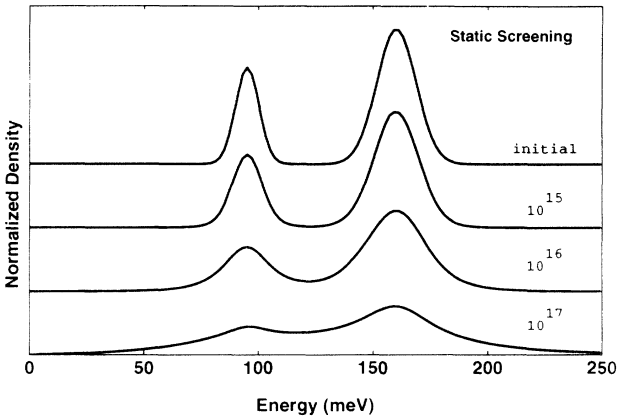

FIG. 5. The initial and final distribution of photoexcited electrons, calculated as in Fig. 3, but with static screening.

CCS becomes significant because the calculations use the band-edge electron effective mass. By neglecting conduction band nonparabolicity, the calculations fail to take into account the mass mismatch between the energetic electrons and the electrons in the cool plasma, and as a result they overestimate the scattering of the energetic electrons. The mass mismatch is expected to be significant in the experiment by Kash, where the electron energy is 300 meV, and the "slope" effective mass at this energy is approximately 1.3 times the band-edge effective mass.[11] Our results in Sec. III C 1 do not require correction for the use of the band-edge mass, since no significant mass mismatch exists among the photoexcited electrons.

Our calculations do not consider the plasmon scattering that can occur when an energetic carrier is immersed in a cool plasma. However, an analysis of $\epsilon_{\mathrm{RPA}}(\mathbf{q},\omega)$ by Sato and Hori showed that at a density of 10^{18} cm^{-3} the plasmon modes in a 300 K Maxwell-Boltzmann plasma are strongly damped, and energetic electrons lose much less energy through plasmon emission than through binary collisions with electrons.[32] Since plasmon scattering becomes less important as the plasma density is reduced, we expect plasmon scattering to be even less significant at densities of 10^{15} to 10^{17} cm^{-3}, in spite of the reduced plasmon damping in a 100 K plasma compared to a 300 K plasma. The importance of plasmon scattering is further reduced if Landau damping of the plasmon by intervalence transitions is considered.[34]

3. *Dynamic vs static screening*

For comparison, calculations were also performed using the static dielectric function $\epsilon(\mathbf{q},0)$, obtained by setting $\omega = 0$ in Eq. (5). Results for scattering without and with a 100 K background plasma are shown in Figs. 5 and 6, respectively. Figures 3 and 5 permit a comparison of dynamic and static models for scattering among photoexcited carriers, and Figs. 4 and 6 permit a comparison for scattering in a cool background. The static model underestimates the effects of CCS on the photoexcited electrons, particularly at higher densities. The underestimate does not arise as a result of the lattice being treated statically; since the carrier-carrier interactions at our densities involve energy exchanges much lower than the LO-phonon energy, there is no effect if the frequency-dependent lattice dielectric function comprising the first two terms in Eq. (5) is replaced by ϵ_0, its static limit. Rather, the reason the static dielectric function $\epsilon(\mathbf{q},0)$ causes CCS to be underestimated is the way it treats screening by the carriers. We noted in Sec. I that static screening will be a poor approximation for any collision where the center-of-mass velocity is on the order of, or greater than, the velocity of the screening carriers.[29] When an energetic electron scatters from another carrier, the surrounding holes usually have a lower velocity than the center of mass of the two colliding carriers. Therefore we find that static screening by holes is a poor approximation, whether the holes are photoinjected or are part of a cool plasma. Similarly, we observe that static screen-

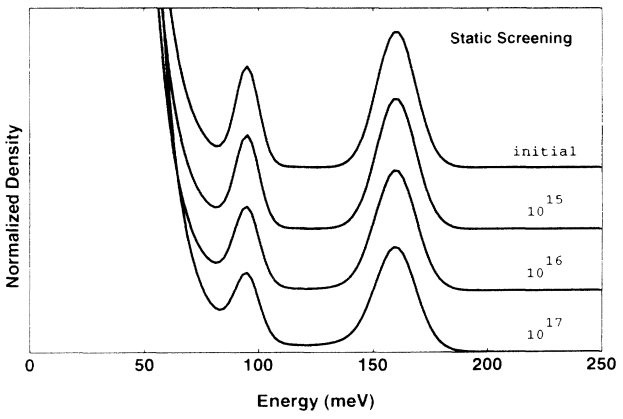

FIG. 6. The initial and final distribution of photoexcited electrons immersed in a 100 K Maxwell-Boltzmann plasma, calculated as in Fig. 3, but with static screening.

ing by electrons is a poor approximation when the electrons are part of a cool plasma. In both cases the static model overestimates the screening and therefore causes the effects of the scattering to be underestimated. However, for scattering among photoexcited carriers in the absence of a cool plasma, treating the screening by the excited electrons statically causes the effects of CCS to be *overestimated*. The overestimate arises because, unlike an equilibrium distribution, a shell-like distribution has a susceptibility $\chi(\mathbf{q},\omega)$ whose maximum magnitude (maximum screening) does not occur at $\omega = 0$ but at $0 < \omega < \omega_p$. For the electron susceptibility, the maximum occurs at an energy $\hbar\omega$ in the range of frequent collisional energy transfers between electrons. (In this respect the RPA dielectric function is qualitatively different from the less accurate plasmon-pole dielectric function used in previous dynamically screened Boltzmann calculations.[13,38,39])

Therefore when a static screening model is applied to scattering among photoexcited carriers, the scattering is underestimated because of the static treatment of screening by holes, but this is partially compensated by the static treatment of screening by electrons. For the case of an energetic electron in a cool plasma, the scattering rate is underestimated as a result of statically treating the screening by both carrier types.

IV. CONCLUSION

In conclusion, we have studied carrier-carrier scattering in photoexcited electron-hole plasmas using two nonequilibrium methods that include dynamic screening: numerical solution of the dynamically screened Boltzmann equation and molecular dynamics. We have found that molecular dynamics is dominated by nonphysical effects at short times, arising from the pointlike nature of the simulated carriers. Solution of the Boltzmann equation with dynamic screening, however, indicates that in the absence of a cool background carrier-carrier scattering is as significant as LO-phonon emission for the scattering of energetic electrons at pair densities greater than about 8×10^{15} cm^{-3}, and at 10^{17} cm^{-3} the photoexcited electrons are nearly thermalized in 150 fsec. These results are in agreement with previous experimental data. The interaction between carriers has a stronger effect in this case than when a low density of energetic electrons is immersed in a cool background, where previous work has shown that carrier-carrier scattering is not significant until a plasma density of approximately 8×10^{16} cm^{-3} is reached. We attribute the stronger effect of carrier-carrier scattering in the absence of a cool background to the fact that screening is weaker in an energetic photoexcited distribution than in a cool thermal one. This conclusion could be tested with a pump-probe experiment in which a low density of electrons generated by a probe pulse scatters from the plasma generated by a pump pulse, as in Ref. 5, but using pulse lengths ≤ 150 fsec, with a variable time delay between pump and probe to adjust the time available for thermalization (and therefore the average energy) of the plasma experienced by the probe carriers. In addition, a two-color femtosecond pump-probe experiment would allow the distribution of the pump plasma to have its average energy and its shape varied independently. This would permit the dependence of screening on the average energy of the screening distribution to be evaluated separately from its dependence on the shape of the screening distribution.

ACKNOWLEDGMENTS

We would like to thank R. Bhatt, D. Snoke, N. Wingreen, and P. Wolff for helpful discussions. This work was supported in part by the Advanced Technology Center for Photonics and Optoelectronic Materials established by Princeton University and the State of New Jersey, and by the Army Research Office under Grant No. DAAL03-92-G-0146. The calculations were further supported by Digital Equipment Corp. under a DEC-DPRI Grant, and by the National Science Foundation under Grant No. CDA-9121709.

[1] D. N. Mirlin, I. Ya. Karlik, L. P. Nikitin, I. I. Reshina, and V. G. Sapega, Solid State Commun. **37**, 757 (1981).
[2] W. Fawcett, A. D. Boardman, and S. Swain, J. Phys. Chem. Solids **31**, 1963 (1970).
[3] B. P. Zakharchenya, D. N. Mirlin, V. I. Perel', and I. I. Reshina, Usp. Fiz. Nauk **136**, 459 (1982) [Sov. Phys. Usp. **25**, 143 (1982)].
[4] J. A. Kash, J. M. Hvam, and J. C. Tsang, Phys. Rev. Lett. **54**, 2151 (1985).
[5] J. A. Kash, Phys. Rev. B **40**, 3455 (1989).
[6] J. F. Young, N. L. Henry, and P. J. Kelly, Solid-State Electron. **32**, 1567 (1989).
[7] J. F. Young, P. J. Kelly, N. L. Henry, and M. W. C. Dharma-wardana, Solid State Commun. **78**, 343 (1991).
[8] K. W. Sun, M. G. Kane, and S. A. Lyon, Europhys. Lett. **26**, 123 (1994).
[9] T. Elsaesser, J. Shah, L. Rota, and P. Lugli, Phys. Rev. Lett. **66**, 1757 (1991).
[10] D. W. Snoke, Phys. Rev. B **47**, 13 346 (1993).
[11] J. S. Blakemore, J. Appl. Phys. **53**, R123 (1982).
[12] P. Lugli and D. K. Ferry, Physica B+C **134B**, 364 (1985).
[13] S. Hunsche, H. Heesel, A. Ewertz, H. Kurz, and J. H. Collet, Phys. Rev. B **48**, 17 818 (1993).
[14] L. Rota and P. Lugli, Semicond. Sci. Technol. **7**, B180 (1992).
[15] C. J. Stanton, D. W. Bailey, and K. Hess, IEEE J. Quantum Electron. **24**, 1614 (1988).
[16] C. Kiener, G. Zandler, and E. Vass, Solid State Commun. **65**, 1241 (1988).
[17] S. M. Goodnick and P. Lugli, Phys. Rev. B **37**, 2578 (1988).
[18] A. Matulionis, J. Pozela, and A. Reklaitis, Solid State Commun. **16**, 1133 (1975).
[19] P. Lugli and D. K. Ferry, Physica B+C **117B&118B**, 251 (1983).

[20] M. A. Osman and D. K. Ferry, Phys. Rev. B **36**, 6018 (1987).
[21] J. F. Young, P. Kelly, and N. L. Henry, Phys. Rev. B **36**, 4535 (1987).
[22] L. Rota and P. Lugli, Solid-State Electron. **32**, 1423 (1989).
[23] R. P. Joshi, R. O. Grondin, and D. K. Ferry, Phys. Rev. B **42**, 5685 (1990).
[24] S. E. Guncer and D. K. Ferry, Semicond. Sci. Technol. **7**, B324 (1992).
[25] D. W. Snoke, W. W. Rühle, Y.-C. Lu, and E. Bauser, Phys. Rev. B **45**, 10 979 (1992).
[26] P. Lugli and D. K. Ferry, IEEE Electron Device Lett. **EDL-6**, 25 (1985).
[27] P. Lugli and D. K. Ferry, Appl. Phys. Lett. **46**, 594 (1985).
[28] U. Hohenester, P. Supancic, P. Kocevar, X. Q. Zhou, U. Lemmer, G. C. Cho, W. Kütt, and H. Kurz, Semicond. Sci. Technol. **7**, B176 (1992).
[29] J. R. Meyer and F. J. Bartoli, Phys. Rev. B **28**, 915 (1983).
[30] M. E. Kim, A. Das, and S. D. Senturia, Phys. Rev. B **18**, 6890 (1978).
[31] J. M. Rorison and D. C. Herbert, J. Phys. C **19**, 3991 (1986).
[32] H. Sato and Y. Hori, Phys. Rev. B **36**, 6033 (1987).
[33] C. L. Petersen and S. A. Lyon, Phys. Rev. Lett. **65**, 760 (1990).
[34] J. F. Young, P. J. Kelly, and N. L. Henry, Semicond. Sci. Technol. **7**, B148 (1992).
[35] P. M. Platzmann and P. A. Wolff, *Waves and Interactions in Solid State Plasmas* (Academic, New York, 1973), Chap. 2.
[36] P. Lugli and D. K. Ferry, Phys. Rev. Lett. **56**, 1295 (1986).
[37] M. J. Kann, A. M. Kriman, and D. K. Ferry, Phys. Rev. B **41**, 12 659 (1990).
[38] J. Nunnenkamp, J. H. Collet, J. Klebniczki, J. Kuhl, and K. Ploog, Phys. Rev. B **43**, 14 047 (1991).
[39] J. H. Collet, Phys. Rev. B **47**, 10 279 (1993).
[40] L. I. Schiff, *Quantum Mechanics*, 3rd ed. (McGraw-Hill, New York, 1968).
[41] J. D. Jackson, *Classical Electrodynamics*, 2nd ed. (Wiley, New York, 1975), Chap. 13.
[42] T. Morita, Prog. Theor. Phys. **22**, 757 (1959).
[43] A. A. Barker, J. Chem. Phys. **55**, 1751 (1971).
[44] H. Minoo, M. M. Gombert, and C. Deutsch, Phys. Rev. A **23**, 924 (1981).
[45] J. P. Hansen and I. R. McDonald, Phys. Rev. A **23**, 2041 (1981); L. Sjögren, J. P. Hansen, and E. L. Pollock, *ibid.* **23**, 2041 (1981); B. Bernu and J. P. Hansen, Phys. Rev. Lett. **48**, 1375 (1982).
[46] R. Car and M. Parrinello, Phys. Rev. Lett. **55**, 2471 (1985).
[47] J. Clérouin, G. Zérah, D. Benisti, and J. P. Hansen, Europhys. Lett. **13**, 685 (1990).
[48] A. M. Kriman, M. J. Kann, and D. K. Ferry, Phys. Rev. Lett. **65**, 1619 (1990)
[49] A. M. Kriman, R. P. Joshi, M. J. Kann, and D. K. Ferry, Semicond. Sci. Technol. **7**, B243 (1992)
[50] N. Bohr, K. Dan. Vidensk. Selsk. Mat.-Fys. Medd. **XVIII**, No. 8 (1948).
[51] H. Ehrenreich and M. H. Cohen, Phys. Rev. **115**, 786 (1959).
[52] X. Q. Zhou, K. Leo, and H. Kurz, Phys. Rev. B **45**, 3886 (1992).
[53] D. Pines and D. Bohm, Phys. Rev. **85**, 338 (1952).
[54] A. I. Akhiezer, I. A. Akhiezer, R. V. Polovin, A. G. Sitenko, and K. N. Stepanov, *Collective Oscillations in a Plasma* (MIT Press, Cambridge, MA, 1967), Sec. 12.
[55] J. B. Stark and P. A. Wolff, Solid-State Electron. **32**, 1327 (1989).
[56] J. D. Wiley, Phys. Rev. B **4**, 2485 (1971).
[57] J. Lindhard, K. Dan. Vidensk. Selsk. Mat.-Fys. Medd. **28**, No. 8 (1954).
[58] D. W. Snoke and J. P. Wolfe, Phys. Rev. B **39**, 4030 (1989).